Journal of Additive Manufacturing Technologies
DOI: 10.18416/JAMTECH.2212648

Infinite Science | Publishing

Mechanical behavior and microstructural characterization of wire and arc additive manufacturing of er70s-6 low carbon steel alloy

M. Abbaszadeh[1], N. Bol[1], O. Ece Kara[1], A. A. Sen[1], and O. Yılmaz[2]*

[1]INTECRO Robotics company, Ankara, Turkey, Masoud.abbaszadeh@intecro.com.tr
[2]Advanced Manufacturing Technology Research Group (AMTRG), Gazi University, Ankara, Turkey,
** Corresponding author, email: oguzhanyilmaz@gazi.edu.tr*

Abstract

Wire and Arc Additive Manufacturing (WAAM) is relatively a novel manufacturing technology which uses metallic wire as the feedstock material and normal arc as the heat source to build up large scale near-net-shape parts. This process has attracted the attention of many industries such as aerospace, defense and automotive due to its ability to produce very near-net-shape components without complex tooling and molds offers potential for significant cost and lead time reductions. In this paper, the mechanical and metallurgical properties of the WAAM ER70S-6 are studied during tension loading as well as microhardness testing and its behavior is correlated with microstructural observations. The microstructure of WAAM ER70S-6 is assessed by optical microscopy (OM). The results show that the selected parameters for deposition of ER70S-6, leads to an isotropic mechanical behavior during tension loading. The microhardness level is not changing in different regions of WAAM-fabricated ER70S-6, confirming presence of relatively homogenous microstructure.

Keywords: WAAM, tension loading, optical microscopy, microhardness.

1. Introduction

Wire and Arc Additive Manufacturing (WAAM) is a cost-effective additive manufacturing (AM) technology that produces 3D metallic components by depositing thin layers of metals in a layer-by-layer fashion. Compared to other AM technologies, WAAM process is using metal wire instead of powder which is 90% cheaper than the latter one [1], and arc as the heat source instead of laser or electron beam. In addition, this process has the highest deposition rate (up to 8 kg/h) compared to other AM technologies such as electron beam and laser deposition [2] that enables it to fabricate components with no dimensional limits [3] in shorter time; the manufacturing time is reduced up to 60% by WAAM process [4]. In recent years, different materials such as aluminum alloys [5], titanium [6], and steel alloys [7] have been successfully processed by WAAM process.

During WAAM process, the metal wire is melted by electric arc and deposited on the substrate or already solidified part. This procedure continues until the fabrication of the desired component is completed. Due to the layer-by-layer production strategy of the WAAM process, every region of the material is subjected to the fast and cyclic re-heating and re-cooling. This complex and cyclic thermal history might result in poor geometry of the deposited structure [8], anisotropic mechanical properties [9, 10], and inhomogeneous microstructure [11]. The effect of thermal cycling on the mechanical properties and microstructure distribution of WAAM-fabricated components has been previously reported in the literature [12, 13]. Sridharana et al. [14] studied the mechanical properties and microstructural features of WAAM-fabricated ER70S-6. They reported that the mechanical performance of WAAM-fabricated ER70S-6 shows anisotropic behavior during tensile testing in deposition and building directions. Different grain structures are formed in different regions of WAAM-fabricated ER70S-6 that is originated from different cooling rates in various areas. They particularly found that the building mild steel structural parts using high heat input leads to lower defects such as inter layer lack of fusion and process-induced porosity that results in lower anisotropy in mechanical properties. Similar results were observed by Haden et al. [15] that shows approximately anisotropic mechanical properties in different directions of WAAM-fabricated ER70S-6 mild steel during tension loading.

In this study, the mechanical properties as well as micro-structure of WAAM-fabricated ER70S-6 low carbon steel alloy were investigated by means of mechanical tests such as tensile and microhardness testing and micro-structural evaluations such as optical microscopy (OM). To study the possible anisotropy in WAAM-fabricated ER70S-6, the tensile specimens were cut and tested in two different orientations, i.e., longitudinal (deposition) and normal (building) directions. Moreover, to see the effect of different cooling rates, the microhardness was assessed in three different zones of WAAM-fabricated ER70S-6, i.e., top, middle and bottom regions.

2. Material and methods

2.1. Material deposition process

In the current study, ER70S-6 filler wire with diameter of 1.2 mm was used to build a thin wall-shape structure with dimension of 230×9×195 mm3 using wire and arc additive manufacturing process. To build such a structure, 110 layers of ER70S-6 with average layer height of 1.8 mm were deposited in a zigzag direction. It should be noted that the linear wall was constructed manually, without the use of computer-aided manufacturing (CAM) software. The robot's movement was programmed through the use of a teach pendant, with the robot following a predetermined movement path and depositing the material layer by layer, in accordance with the operator's instructions. ASTM A52 mild steel with dimension of 300×200×30 mm3 was used as the substrate; the substrate was wire brushed and cleaned using acetone to remove any organic contamination and prevent subsequent gas pores formation during the process. A KUKA (KR6 R 1820 ARC HW) 6-axis industrial robot equipped with Fronius TPSi 500 welding power supply and a Fronius CMT torch was employed as the heat source for wire and arc additive manufacturing of the part, see Fig 1a. It should be mentioned that the torch was hold vertical to the substrate during the deposition. It is shown in the literature that the cold metal transfer (CMT) method has the lowest heat input compared to other arc heat sources [16, 17].

Table 1. Chemical composition of ER70S-6 filler wire (wt%).

C	Si	Mn	P	S	Cr
0.13	0.7	1.16	0.0103	0.025	0.025
Mo	Ni	Cu	V	Fe	
0.01	0.03	0.1	0.002	Bal.	

Table 2. The WAAM process parameters to deposit a thin wall using ER70S-6 filler wire.

Parameter	Value
Arc Current	166 A
Arc Voltage	15.3 V
Wire Feed Speed	4.7 m/min
Torch Travel Speed	0.45 m/min
Gas Type	%93 Ar, %2 O_2 %5 CO_2
Gas Flow	18 L/min
Contact Tip to Work Distance	1.78 mm
Cooling Time	90 s

However, in order to avoid excessive heat accumulation during the deposition process, 90 s waiting time was incorporated prior to the deposition of new layer. The process parameters of the WAAM deposition are shown in Table 2. It should be mentioned that the listed parameters in Table 2 for depositing the ER70S-6 filler wire was selected based on a preliminary study that was leading to a minimum level of porosity in the structure as well as higher surface quality of the wall.

2.2. Mechanical properties measurements

Following the deposition process, 1.5 mm of the material was initially removed from each side of the wall using CNC machining to eliminate the surface roughness of the as-deposited wall. Then, the relevant samples for mechanical testing as well as microstructural characterization were cut using wire cutting. It should be emphasized that no additional post-processing was conducted on the WAAM-fabricated wall, and samples for both mechanical and microstructural testing were extracted directly from the as-built structure. Although the machining process may have influenced the resulting hardness of the material near the machined surface, it is important to emphasize that the microstructure and microhardness were evaluated solely in the middle of the samples, rather than at the machined surfaces. In Figure 1b, the schematic of WAAM-fabricated thin wall and the relevant extracted samples are shown.

In order to assess the mechanical properties of the WAAM-fabricated ER70S-6 during tension loading, the tensile specimens according to TS EN ISO 68-92-1 standard with a total length of 120 mm, a gauge length of 32 mm, and a thickness of 6 mm was prepared and tested at room temperature and deformation velocity of 0.25 mm/s. In order to investigate the possible anisotropic behavior of the WAAM-fabricated ER70S-6 during tensile testing, the specimens were cut from both longitudinal and normal directions. The longitudinal and normal directions are parallel to the deposition and building directions, respectively, and the transverse direction is perpendicular to the longitudinal-normal plane. In order to ensure statistical significance of the results and observed trends, tensile testing was performed three times for each tested direction.

The HIGHWOOD (Japan, model HWMMT-X3) Vickers hardness testing machine was used to measure the microhardness of WAAM-fabricated ER70S-6. Thirteen measurements were conducted in the normal-transverse cross-section and from different regions of the WAAM sample, i.e., top, middle and bottom zones with the applied load of 0.3 kg and an indentation time of 45 s. It should be mentioned that the indentation distances were chosen to be 500 μm.

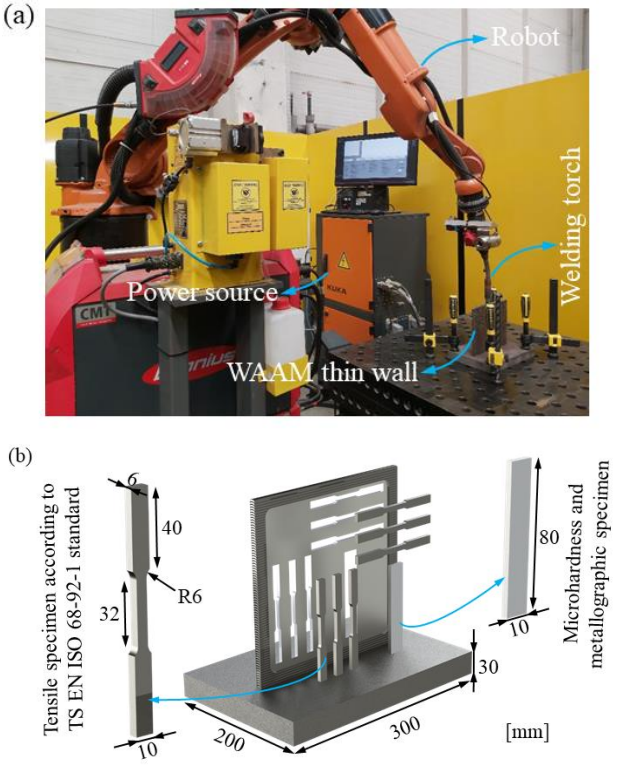

Fig 1. (a) Experimental setup for robot-assisted wire and arc additive manufacturing (WAAM), and (b) Schematic of WAAM-fabricated ER70S-6 thin wall and the relevant tensile and metallographic samples. In order to study the possible anisotropic behavior of the structure, the tensile specimens were extracted and tested in both deposition and building directions.

2.3. Microstructural characterization

The sample for microstructural examination was cut from the normal-transverse plane of the as-received WAAM-fabricated ER70S-6. The sample was firstly mounted, ground subsequently using a series of silicon carbide grinding papers with decreasing coarseness from 1500 grit, and polished by diamond suspension polishing of 6µm, 3µm, and 1µm, respectively. At the final stage, the finely polished sample was etched by immersing the specimen in a 5% Nital reagent (5% nitric acid and 95% ethanol) for 5 s at room temperature. Micro and macro images of etched sample was later obtained using optical microscope (OM) Leica DMI5000 M (Leica Microsystems GmbH, Wetzlar, Germany) to describe microstructural features at different areas.

3. Results and discussion

3.1. Mechanical properties measurements

The stress-strain response of the WAAM-fabricated ER70S-6 low carbon steel alloy during the tensile loading at 0.25 mm/s in both longitudinal (deposition) and normal (building) directions are plotted in Figure 2. Moreover, the corresponding mechanical properties such as yield strength (σ_y), ultimate tensile strength (UTS), and elongation at failure are summarized in Table 3. It is shown that the WAAM-fabricated ER70S-6 steel alloy shows nearly isotropic mechanical properties during tensile testing in longitudinal and normal directions; the mean value of the yield strength, ultimate tensile strength and elongation are 357 MPa, 482 MPa and 31%, respectively. It should be mentioned that similar results in terms of isotropic behavior of the WAAM-fabricated ER70S-6 steel alloy during tensile testing have been reported in the literature [18-20]. Shassere et al. [21] showed that the yield strength of samples extracted from the steady-state area of the thin wall of WAAM-fabricated ER70S-6 in all three directions, e.g., longitudinal, 45° to longitudinal and normal directions remains in the similar range of 360±7 MPa. The UTS is also reported to be in the range of 475±4 MPa in all three aforementioned directions of the steady-state region. The resulting isotropic behavior indicates that the selected parameters for fabrication of WAAM ER70S-6 as well as the chosen cooling time prior to deposition generates reliable and consistent mechanical properties.

In Figure 3, the microhardness test results of WAAM-fabricated ER70S-6 in the longitudinal-normal cross-section and through the normal direction are shown in different zones, i.e., bottom, middle and top zones. It is shown that the microhardness is changing in different zones of the WAAM-fabricated ER70S-6 and through the normal direction. The microhardness is changing from the minimum value of 160 HV to the maximum value of 180 HV. During WAAM process, different regions of the solidified material experiences various cooling rates. This results in the presence of different grain sizes and phases that leads to the changes in the microhardness level [22].

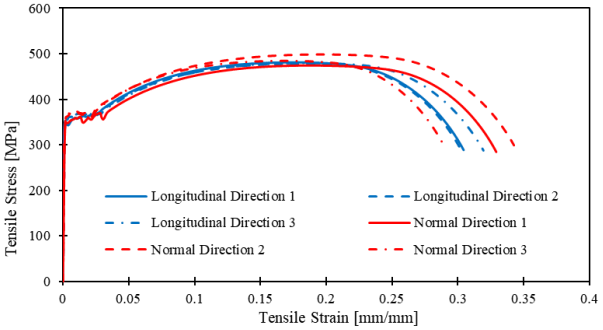

Fig 2. Stress-strain response of WAAM-fabricated ER70S-6 during tensile testing at loading speed of 0.25 mm/s. In order to assess the possible anisotropy in the structure, tensile tests were carried out in both longitudinal (deposition) and normal (building) directions.

Table 3. The mean value and corresponding standard deviation of mechanical properties of WAAM-fabricated ER70S-6 during tension loading at 0.25 mm/s for both longitudinal and normal directions.

Test Direction	Yield Strength [MPa]	Ultimate Strength [Mpa]	Elongation [%]
Longitudinal	356.5±7.5	479.5±1.3	30±0.8
Normal	357.3±6.5	485±10	32±2

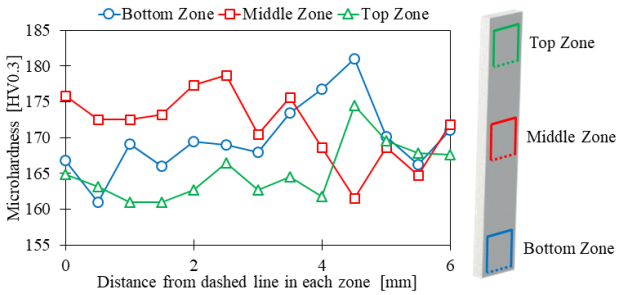

Fig 3. Vickers microhardness test results through the building direction of as-deposited WAAM-fabricated ER70S-6. The starting points of the measurements for each zone are indicated by the dashed line in the figure.

3.2. Microstructural characterization

The low magnification optical microscope images of the WAAM-fabricated ER70S-6 through the building direction is shown in Figure 4a. This figure reveals that the dominant microstructure in the WAAM-fabricated ER70S-6 is equiaxed primary ferrite grains which are bonded within the secondary phase of lamellar pearlite phases. The microstructure contains fine and coarse-grained regions which represent the inner-layer and inter-layer regions, respectively [23]. The higher magnification of optical microscope images from different regions, i.e., fine and coarse-grained regions, of the WAAM-fabricated ER70S-6 is also shown in Figure 4b and c, respectively. It can be seen in this figure that the grain size is changing in the aforementioned WAAM-fabricated ER70S-6 structure. In addition, the amount of secondary phase of pearlite is different in the fine-grained region compared to coarse-grained one. The higher fraction of pearlite phase in the fine-grained region is ascribed to the higher cooling rate of this region that occurs during WAAM process [24].

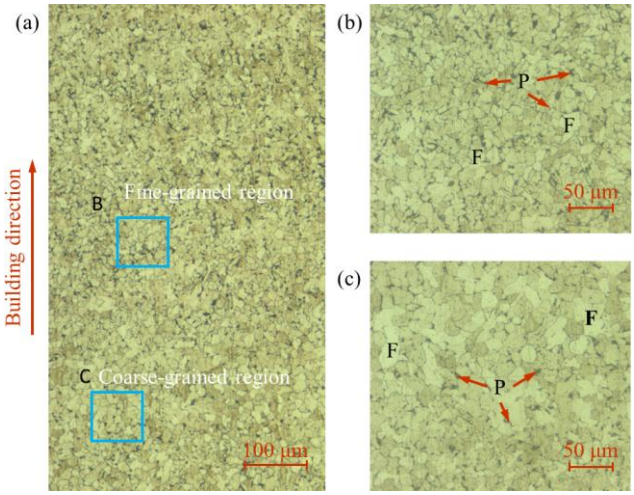

Fig 4. Optical microscope images taken from the WAAM-fabricated ER70S-6, (a) low magnification through the building direction, (b) higher magnification of the enclosed area B, (c) higher magnification of the enclosed area C.

The presence of fine microstructure as well as higher amount of pearlite phase in the fine-grained region of WAAM-fabricated ER70S-6 has also effect on the higher value of the microhardness in this region. It should be mentioned that the obtained microstructure in this study is typical microstructure reported in the previous studies of WAAM-fabricated ER70S-6 [15, 19, 20] as well as low carbon steel, e.g., ST-37 alloy [25].

4. Conclusions

This paper presents an investigation of the mechanical properties and microstructure of wire and arc additive manufacturing (WAAM) of ER70S-6 steel alloy. The results of the study indicate that the parameters selected for the manufacturing process produce relatively isotropic mechanical behavior of the WAAM-fabricated ER70S-6 during tensile testing. Additionally, the microstructure of the WAAM-fabricated ER70S-6 is characterized by equiaxed ferrite grains that are uniformly distributed throughout different regions of the structure, including the inter-layer and inner-layer regions. The microstructure is also comparatively homogeneous. However, the microhardness values fluctuate along the building direction due to small deviations in grain sizes across various regions of the WAAM-fabricated ER70S-6.

Acknowledgments

This work has received funding from the Scientific and Technological Research Council of Turkey (TÜBITAK) under the Grant Agreement No: 3200280 which is gratefully acknowledged.

Author's statement

Conflict of interest: Authors state no conflict of interest. Informed consent: Informed consent has been obtained from all individuals included in this study. Ethical approval: The research related to human use complies with all the relevant national regulations, institutional policies and was performed in accordance with the tenets of the Helsinki Declaration, and has been approved by the authors' institutional review board or equivalent committee.

References

1. Wang, L., Xue, J., Wang, Q., Correlation between arc mode, microstructure, and mechanical properties during wire arc additive manufacturing of 316L stainless steel. Materials Science & Engineering A, 2019. 751: p. 183-190.
2. Liberini, M., Astarita, A., Campatelli, G., Scippa, A., Montevecchi, F., Venturini, G., Durante, M., Boccarusso, L., Minutolo, F.M.C., Squillace, A., Selection of optimal process parameters for wire arc additive manufacturing. Procedia CIRP, 2017. 62: p. 470-474.
3. Derekar, K.S., A review of wire arc additive manufacturing and advances in wire arc additive manufacturing of aluminium. Materials Science and Technology, 2018. 34(8): p. 895-916.
4. Zhao, Y., Jia, Y., Chen, S., Shi, J., Li, F., Process planning strategy for wire-arc additive manufacturing: Thermal behavior considerations. Additive Manufacturing, 2020. 32: p. 100935.
5. Gu, J., Ding, J., Williams, S.W., Gu, H., Bai, J., Zhai, Y., Ma, P., The strengthening effect of inter-layer cold working and post-deposition heat treatment on the additively manufactured Al–6.3Cu alloy. Materials Science and Engineering: A, 2016. 651: p. 18-26.
6. Wang, F., Williams, S.W., Colegrove, P., Antonysamy, A.A., Microstructure and mechanical properties of wire and arc additive manufactured Ti-6Al-4V. Metallurgical and Materials Transactions A, 2013. 44: p. 968-977.

7. Yilmaz, O., Ulga, A.A., Microstructure characterization of SS308LSi components manufactured by GTAW-based additive manufacturing: shaped metal deposition using pulsed current arc. The International Journal of Advanced Manufacturing Technology, 2017. 89: p. 13-25.
8. Wu, B., Pan, Z., Ding, D., Cuiuri, D., Li, H., Effects of heat accumulation on microstructure and mechanical properties of Ti6Al4V alloy deposited by wire arc additive manufacturing. Additive Manufacturing, 2018. 23: p. 151-160.
9. Sun, L., Jiang, F., Huang, R., Yuan, D., Guo, C., Wang, J., Anisotropic mechanical properties and deformation behavior of low-carbon high-strength steel component fabricated by wire and arc additive manufacturing. Materials Science and Engineering: A, 2020. 787: p. 139514.
10. Abbaszadeh, M., Ventzke, V., Neto, N., Riekehr, S., Martina, F., Kashaev, N., Hönnige, J., Williams, S.W., Klusemann, B., Compression behaviour of wire + arc additive manufactured structures. Metals, 2021. 11(6): p. 877.
11. Chen, F., Yang, Y., Feng, H., Regional control and optimization of heat input during CMT by wire arc additive manufacturing: modeling and microstructure effects. Materials, 2021. 14(5): p. 1061.
12. Köhler, M., Hensel, J., Dilger, K., Effects of thermal cycling on wire and arc additive manufacturing of al-5356 components. Metals, 2020. 10(7): p. 952.
13. Ge, J., Ma, T., Han, W., Yuan, T., Jin, T., Fu, H., Xiao, R., Lei, Y., Lin, J., Thermal-induced microstructural evolution and defect distribution of wire-arc additive manufacturing 2Cr13 part: Numerical simulation and experimental characterization. Applied Thermal Engineering, 2019. 163: p. 114335.
14. Sridharan, N., Noakes, M.W., Nycz, A., Love, L.J., Dehoff, R.R., Babu, S.S., On the toughness scatter in low alloy C-Mn steel samples fabricated using wire arc additive manufacturing. Materials Science and Engineering: A, 2018. 713: p. 18-27.
15. Haden, C.V., Zeng, G., Carter, F.M., Ruhl, C., Krick, B.A., Harlow, D.G., Wire and arc additive manufactured steel: Tensile and wear properties. Additive Manufacturing, 2017. 16: p. 115-123.
16. Fang, X., Zhang, L., Chen, G., Dang, X., Huang, K., Wang, L., Lu, B., Correlations between microstructure characteristics and mechanical properties in 5183 aluminium alloy fabricated by wire-arc additive manufacturing with different arc modes. Materials, 2018. 11(11): p. 2075.
17. Lee, S.H., Optimization of cold metal transfer-based wire arc additive manufacturing processes using gaussian process regression. Metals, 2020. 10(4): p. 461.
18. Rafieazad, M., Ghaffari, M., Nemani, A.V., Nasiri, A., Microstructural evolution and mechanical properties of a low-carbon low-alloy steel produced by wire arc additive manufacturing. The International Journal of Advanced Manufacturing Technology, 2019. 105(4): p. 2121-2134.
19. Nemani, A.V., Ghaffari, M., Nasiri, A., On the post-printing heat treatment of a wire arc additively manufactured ER70S part. Materials, 2020. 13(12): p. 2795.
20. Ron, T., Levy, G.K., Dolev, O., Leon, A., Shirizly, A., Aghion, E., The effect of microstructural imperfections on corrosion fatigue of additively manufactured ER70S-6 alloy produced by wire arc deposition. Metals, 2020. 10(1): p. 98.
21. Shassere, B., Nycz, A., Noakes, M.W., Masuo, C., Sridharan, N., Correlation of microstructure and mechanical properties of metal big area additive manufacturing. Applied Sciences, 2019. 9(4): p. 787.
22. Le, V.T., Mai, D.S., Hoang, Q.H., Effects of cooling conditions on the shape, microstructures, and material properties of SS308L thin walls built by wire arc additive manufacturing. Materials Letters, 2020. 280: p. 128580.
23. Colegrove, P.A., Coules, H.E., Fairman, J., Martina, F., Kashoob, T., Mamash, H., Cozzolino, L.D., Microstructure and residual stress improvement in wire and arc additively manufactured parts through high-pressure rolling. Journal of Materials Processing Technology, 2013. 213(10): p. 1782-1791.
24. Hui, W., Zhang, Y., Shao, C., Chen, S., Zhao, X., Dong, H., Effect of cooling rate and vanadium content on the microstructure and hardness of medium carbon forging steel. Journal of Materials Science & Technology, 2016. 32(6): p. 545-551.
25. Ron, T., Levy, G.K., Dolev, O., Leon, A., Shirizly, A., Aghion, E., Environmental behavior of low carbon steel produced by a wire arc additive manufacturing process. Metals, 2019. 9(8): p. 888.